ISSN 0023-1584, Kinetics and Catalysis, 2008, Vol. 49, No. 3, pp. 407–412. © MAIK "Nauka/Interperiodica" (Russia), 2008.
Original Russian Text © O.V. Udalova, D.P. Shashkin, M.D. Shibanova, O.V. Krylov, 2008, published in Kinetika i Kataliz, 2008, Vol. 49, No. 3, pp. 428–433.

Changes in the Phase Composition of a Multicomponent Co–Mo–Bi–Fe–Sb–K–O Catalyst under Conditions of the Partial Oxidation of Isobutylene to Methacrolein: A Comparison with the Oxidation of Propylene to Acrolein

O. V. Udalova, D. P. Shashkin, M. D. Shibanova, and O. V. Krylov

Semenov Institute of Chemical Physics, Russian Academy of Sciences, Moscow, 117977 Russia

E-mail: korchak@chph.ras.ru

Received October 17, 2005; in final form, October 16, 2007

Abstract—The partial oxidation of isobutylene to methacrolein on a multicomponent multiphase Co–Mo–Bi–Fe–Sb–K–O catalyst and on catalysts from which some components were absent was studied. Activity and selectivity changes in the case of isobutylene oxidation were the same as in the oxidation of propylene; however, the rate of propylene oxidation was higher than that of isobutylene oxidation. The X-ray diffraction analysis of the catalysts before and after the reaction indicated the occurrence of a number of phases in the samples: α-$CoMoO_4$, β-$CoMoO_4$, $Fe_2(MoO_4)_3$, reduced bismuth molybdate species, MoO_3, and reduced MoO_x species. Under catalytic reaction conditions, redox phase transformations occurred. Iron molybdate and molybdenum oxide phases underwent the largest transformations. Of two molybdenum oxide phases, a β-Mo_4O_{11} phase with a structure of a crystallographic shift is formed in the course of catalysis, whereas the second phase (MoO_3) almost does not participate in catalysis and occurs in an excess.

DOI: 10.1134/S0023158408030142

INTRODUCTION

Complex multicomponent oxide catalysts of various compositions based on Bi, Fe, and Co molybdates catalyze the partial oxidation of propylene to acrolein, the oxidative ammonolysis of olefins, and the oxidation of methanol to formaldehyde. Many researchers considered the nature of the activity and selectivity of complex molybdate catalysts. At the Semenov Institute of Chemical Physics, Russian Academy of Sciences, Maksimov et al. [1] proposed a model for the action of a Co–Mo–Bi–Fe–O catalyst for the partial oxidation of olefins. According to this model, a multiphase system is required for the operation of the complex catalyst. Each particular phase is a catalyst for one of the steps of a complex process: oxygen activation, olefin activation, oxygen ion diffusion in the lattice, etc.

A relationship between the crystallographic structure and the catalytic properties of V–Mo oxide catalysts was studied for the oxidative transformations of olefins [2]. A number of phases based on molybdenum oxide were detected. The phase composition changed under the action of catalytic reaction and temperature. A modifying additive of vanadium oxide stabilized the active component—a hexagonal MoO_3 phase. Under reaction conditions, nonstoichiometric MoO_{3n-x} phases were also formed. A monoclinic β-Mo_4O_{11} phase, which participated in catalysis at 360–400°C, was detected. Nonstoichiometric Mo_4O_{11} phase nucleation was also described by Kihlborg [3]. It is believed that this nucleation occurs by the reaction

$$4Fe_2(MoO_4)_3 \Leftrightarrow \beta\text{-}FeMoO_4 + Mo_4O_{11} + 5O_L,$$

where O_L is lattice oxygen.

Previously [4, 5], we studied the crystal structure of a multicomponent Co–Mo–Bi–Fe–K–Sb–O catalyst and its activity and selectivity in the partial oxidation of propylene to acrolein. The structure and activity of catalysts from which some phases of the complex system were absent (Fe or Bi molybdates) were also studied. Because the role of the molybdenum oxide phase was least known among various phases that constitute the complex catalyst, we specially studied the effect of the added amount of MoO_3 on the structure and activity of this catalytic system. In general, the study provided support for previous conclusions [1, 2] on the roles of individual phases. The experimental results demonstrated that molybdenum oxide in oxidized and reduced forms was present in all of the catalysts; it is likely that this oxide participated in the formation of an active surface rather than serving as a simple buffer. The selectivity of the catalyst depended on bismuth molybdates, whereas the activity depended on the oxidized and reduced phases of iron molybdates. The reduction and reoxidation of Bi and Fe molybdates and MoO_x occurred under conditions of catalysis.

In recent years, multicomponent catalysts based on transition element molybdates have been studied in the

oxidative dehydrogenation of lower alkanes, the oxidation of butane to maleic anhydride, and the oxidation of methanol to formaldehyde rather than in the partial oxidation of olefins to unsaturated aldehydes (see reviews [6, 7]). The studies of crystal structure–catalytic activity relationships are in progress. A consideration of the role of various bivalent metal (Co, Ni, and Fe) molybdate structures demonstrated that α-molybdates can be responsible for the high activity of molybdate catalysts and β-molybdates can be responsible for selectivity in partial oxidation. The relative concentrations of β- and α-molybdates affect the ratio between redox processes in a complex system. An excess of the MoO_3 phase increased the rate of a reoxidation step [8, 9]. According to Li et al. [10], the incorporation of molybdenum oxides into the lattice of $Fe_2(MoO_4)_3$ increases catalytic activity; however, there are no direct data on the insertion of MoO_3 into molybdate lattices. Electron-microscopic data indicated that molybdate small crystals occurred over larger MoO_3 crystals. Alkali metal (K and Cs) additives also facilitated catalyst reoxidation; however, unlike MoO_3, alkali metal ions remained on the surface and did not enter into bulk phases in this case.

The activity and selectivity of the Co–Mo–Bi–Fe–K–Sb–O complex catalyst was studied in the oxidation of isobutylene to methacrolein [11, 12]. It was found that selectivity decreased as the iron molybdate phase content of the catalyst was increased, that is, as the amount of active oxygen increased. These phases are responsible for the sorption and activation of oxygen. Bismuth molybdate is a phase responsible for the adsorption of isobutylene. The presence of this phase in the complex catalyst resulted in hindered oxygen transport; because of this, selectivity for acrolein increased. The stepwise mechanism of partial isobutylene oxidation was studied using a pulse technique. Methacrylic acid, propylene, acrolein, CO, and acetic acid were detected in reaction products in addition to methacrolein and CO_2.

In this work, we continued a study of the oxidation of isobutylene to methacrolein on the Co–Mo–Bi–Fe–K–Sb–O complex oxide catalyst, which was studied previously [4, 5] as a catalyst for propylene oxidation to acrolein. The final aim was to determine the roles of individual phases of the multicomponent system in catalysis. Along with the catalyst that contained all of the components corresponding to the specified formula, we also studied systems from which some of the components (Fe or Bi molybdates) were absent, as well as catalysts containing various amounts of molybdenum. As a continuation of previous studies [11, 12], we specially examined the effect of the MoO_3 phase on the activity, selectivity, and structure of the complex catalyst. The experimental results were compared with data for propylene oxidation [4, 5].

EXPERIMENTAL

Catalytic tests were performed in a quartz flow reactor 12 mm in diameter and 120 mm in length with a thermocouple well 5 mm in diameter. A catalyst fraction of particle size 0.5–1 mm was placed on quartz gauze at the bottom part of the reactor. The catalyst bed volume was 1.5 cm^3 (1.02–1.12 g). The free volume of the reactor was filled with broken quartz. A gas mixture was supplied with a gas flow controller, and electric heating was controlled using a Minitherm 300 temperature regulator. The flow rate of the initial mixture of 5% isobutylene in air was 10–30 cm^3/min, which corresponded to a contact time of 3–9 s.

The hot reaction flow passed through the catalyst bed and immediately arrived at a six-way valve to exclude the condensation of high-boiling components. The six-way valve was arranged in a chromatograph oven heated to 140°C in order to switch flows before and after the reactor. Next, the reaction flow was distributed over three six-wave valves with sample loops, which were arranged in the same oven. Analysis for hydrocarbons was performed with the use of a flame-ionization detector and a column 0.4 m in length and 5 mm in diameter packed with Porapak QS at 140°C. Oxygen and carbon monoxide were separated for analysis on a column 2 m in length and 3 mm in diameter packed with molecular sieves 5A at 90° and detected using a thermal-conductivity detector; carbon dioxide was determined on a column 3 m in length and 3 mm in diameter packed with Porapak T at 90° (thermal-conductivity detector).

The concentrations of isobutylene, carbon monoxide, and carbon dioxide were quantitatively evaluated by comparing the chromatographic peaks of reaction mixture samples and specially prepared reference mixtures for each of the above substances. Aqueous solutions of pure acetic and methacrylic acids were used for calibration with these substances. Because of the low stability of methacrolein due to polymerization, a calculation procedure was used based on the conversion of isobutylene on a highly selective catalyst at a reactor temperature that resulted in the practical absence of other reaction products.

The catalysts were prepared in accordance with a procedure described elsewhere [4]. The same catalysts as those described previously [5] were prepared.

X-ray diffraction analysis was performed on a modified DRON-3 X-ray diffractometer (filtered CuK_α radiation). The accuracy of measurements was ±3.5%. Diffraction spectra were compared with reference samples, ASTM data files for powder materials, and published data and treated using a number of mathematical programs. The measurements were performed before and after catalytic activity tests.

The samples were placed in the same cell of amorphous silica 10 mm in diameter and 1 mm in depth. The same catalyst volume was taken for measurements, whereas the catalyst weight changed depending on both

Table 1. Dependence of selectivity on temperature and contact time in the oxidation of isobutylene on the multicomponent catalyst $Co_6Mo_{12}Bi_{0.75}Fe_3Sb_{0.1}K_{0.1}O_x$

Contact time, s	T, °C	$X_{C_4H_8}$, %	$S_{Cé}$, %	S_{CO_2}, %	S_{MA}, %	Y_{MA}, %	S_{MAA}, %	S_{AA}, %	Balance, %
9	320	32.1	0.0	7.6	71.5	23.1	1.0	1.5	94.1
	340	57.4	0.0	11.7	46.5	81.0	1.3	0.1	97.4
	360	93.0	2.5	23.0	66.5	61.8	1.7	1.5	96.2
	380	94.1	4.1	25.6	57.7	54.3	1.6	2.2	91.8
6	320	23.7	0.0	20.8	65.3	15.5	0.7	1.1	96.3
	340	63.8	0.0	8.1	87.7	55.9	1.1	1.1	99.9
	360	96.8	2.5	13.6	79.5	77.0	1.8	1.9	99.4
3	320	13.7	0.0	17.2	85.9	11.7	0.0	1.7	98.5
	340	40.5	0.5	5.7	95.0	36.1	1.3	0.7	99.2
	360	97.8	4.3	5.6	86.0	84.1	1.6	1.7	99.1

Note: X is conversion, S is selectivity, Y is yield, MAA is methacrylic acid, MA is methacrolein, and AA is acetic acid.

the elemental composition of the sample and the degree of packing and dispersity. Crystallite sizes changed only slightly, as judged from the halfwidths of corresponding X-ray peaks.

All of the calculations were performed with reference to the base line of β-$CoMoO_4$ (d = 3.360–3.370 Å) as the most intense line for all of the samples and stable under catalysis conditions. It was noted previously [2, 13] that this phase has the polymorphic modification α-$CoMoO_4$, which is formed from β-$CoMoO_4$ under mechanical action. However, the heating of α-$CoMoO_4$ resulted in the opposite effect, the conversion of the α phase to the β phase:

$$\beta\text{-}CoMoO_4 \underset{\text{temperature}}{\overset{\text{pressure}}{\rightleftharpoons}} \alpha\text{-}CoMoO_4.$$

In some cases, normalization for calculating intensity was performed using the total intensities before and after catalysis. The total intensity was retained to within ±3.5%.

RESULTS AND DISCUSSION

Of the tested catalysts, the $Co_6Mo_{12}Bi_{0.75}Fe_{2.3}Sb_{0.1}K_{0.1}O_x$ catalyst, which was studied previously in the partial oxidation of propylene [5], was most active and selective in the partial oxidation of isobutylene. Table 1 summarizes the results of a study of the dependence of the activity and selectivity of this catalyst on contact time and temperature. The total conversion of isobutylene increased with temperature over the range 320–360°C and changed only slightly with contact time above 340°C. The selectivity for methacrolein (S_{MA}) decreased with contact time. A maximum value of S_{MA} was observed at 340–360°C (contact time of 3–6 s), and a maximum yield of methacrolein (Y_{MA}) was observed at 360°C and a contact time of 3 s. Acrolein and acrylic acid were present in reaction products in addition to methacrolein, CO, CO_2, methacrylic acid, and acetic acid; because of this, the overall balance on products was somewhat lower than 100%.

A comparison with analogous data obtained on the same catalyst for the partial oxidation of propylene to acrolein [4] demonstrated that (1) corresponding characteristics for propylene oxidation were reached at a temperature 20–30 K lower than that for isobutylene oxidation and (2) the selectivity of propylene oxidation to acrolein at 290–350°C was higher than that for isobutylene oxidation to methacrolein.

Next, it was of interest to study the oxidation of isobutylene on catalysts that do not contain a base component of the multicomponent catalyst (Bi or Fe molybdates) and thus to change the conditions of formation of various phases. The removal of bismuth oxide from the catalyst caused a dramatic decrease in methacrolein selectivity: from 80–88 to 24–26% at 320°C and from 54–60 to 8–12% at 380°C. In this case, the conversion of isobutylene increased from 8–10 to 17% at 320°C and from 68 to 92–95% at 380°C. The removal of iron oxide resulted in opposite effects: at 380°C, the selectivity increased to 59–63% and the conversion decreased to 60%. Qualitatively, analogous regularities were also observed in the oxidation of propylene to acrolein: molybdenum oxide and iron molybdate are responsible for activity, whereas bismuth molybdate is responsible for selectivity for unsaturated aldehydes.

We studied activity and selectivity changes in the oxidation of isobutylene to methacrolein depending on the MoO_3 content of the catalyst at 340 and 360°C. The ratio between molybdenum oxide and the other components in the samples was retained equal to that in the most selective Co–Mo–Bi–Fe–O catalyst additionally containing Sb and K (see Table 1). As can be seen in Fig. 1, a maximum selectivity in the oxidation of isobutylene to methacrolein was observed at a molybdenum content of 11–12 atoms (in terms of the empirical formula). The selectivity dramatically increased at a molybdenum content of greater than 12. A maximum activity in the oxidation of isobutylene and the highest yield of methacrolein were found in the Mo_{11} system at 340°C and in the Mo_{12} system at 360°C. The changes

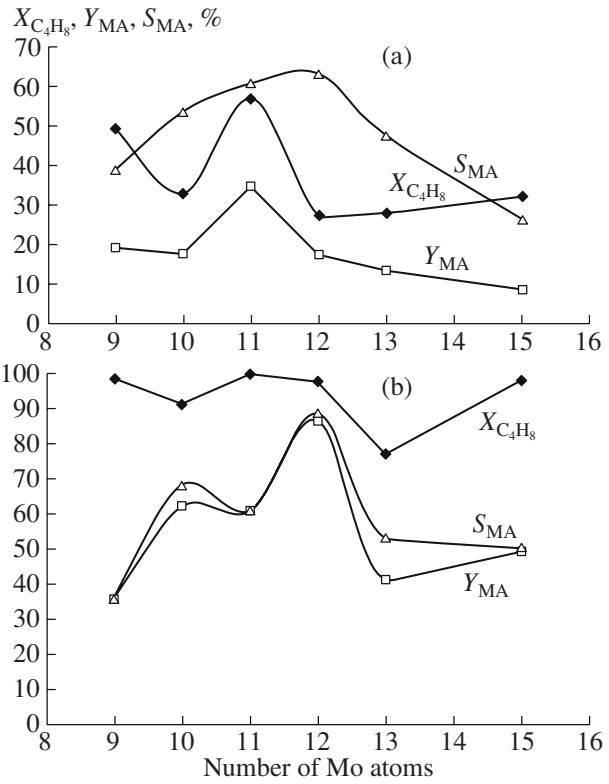

Fig. 1. Isobutylene conversion ($X_{C_4H_8}$), the yield of methacrolein (Y_{MA}), and selectivity for methacrolein (S_{MA}) as functions of the molybdenum content of the Co–Mo–Bi–Fe–O catalyst in isobutylene oxidation at (a) 340 and (b) 360°C.

in activity and selectivity were approximately the same as those in the oxidation of propylene on the same catalysts. However, the overall activity and selectivity were several percent lower and the temperature at which corresponding characteristics for isobutylene oxidation were reached was 10–30 K higher than those for propylene oxidation.

Table 2 summarizes the results of the X-ray diffraction analysis of samples before and after the reaction of isobutylene oxidation performed on these samples. It can be seen in Table 2 that the initial samples consisted of the α and β phases of cobalt molybdate, trivalent iron molybdate $Fe_2(MoO_4)_3$, and rhombic-system bismuth molybdates $Bi_2O_3 \cdot xMoO_3$, where $x = 1–3$. The formation of a nonstoichiometric β-Mo_4O_{11} oxide occurred only in the course of the catalytic reaction in samples with Mo contents of no higher than 12. The formation of this phase almost did not occur as the Mo content was increased. The most detectable amount of this phase was observed in the samples containing 11–12 Mo atoms. These samples exhibited the highest activity in isobutylene oxidation. Under reaction conditions, the phase transformations of Co, Bi, and Fe molybdates occurred along with the reduction of MoO_3.

The experimental data on the redox rearrangement of catalyst phases under catalytic reaction conditions are consistent with the results of our previous studies and with published data [1–12]. The trivalent iron molybdate $Fe_2(MoO_4)_3$ can be converted into bivalent β-$FeMoO_4$, and cobalt molybdate α-$CoMoO_4$ can be converted into β-$CoMoO_4$ [1, 11]. The β-$FeMoO_4$ molybdate is isostructural to β-$CoMoO_4$. The former molybdate is difficult to detect in a complex catalyst by X-ray diffraction analysis because the lattice parameters of both of the molybdates are similar: they are a = 10.21 Å, b = 9.27 Å, and c = 7.02 Å and β = 106°56′ for β-$FeMoO_4$ and a = 10.29 Å, b = 9.39 Å, and c = 7.07 Å and β = 106°31′ for β-$FeMoO_4$ [14]. Therefore, we cannot separate a signal due to β-$FeMoO_4$. Complex structure rearrangements occurred in bismuth molybdates. Under conditions of catalysis, the following three phases were observed: $Bi_2O_3 \cdot MoO_3$, $Bi_2O_3 \cdot 2MoO_3$, and $Bi_2O_3 \cdot 3MoO_3$. In this case, the molybdate with one MoO_3 molecule can be converted into the molybdates with two and three MoO_3 molecules under reaction conditions.

A special feature of the three bismuth molybdates is that the most intense reflections occur within a narrow range of interplanar spacings d = 3.17–3.19 Å. These molybdates were identified with consideration for other interplanar spacings for each particular phase. In the presence of the iron molybdate $Fe_2(MoO_4)_3$, the ternary compound $Bi_2Fe_2Mo_2O_{12}$ can be formed.

Rhombic and hexagonal molybdenum oxides and many nonstoichiometric molybdenum oxide phases, which are absent from the initial samples, play an active role in the redox rearrangements of the catalyst. The simple calcination of the rhombic phase in air resulted in its reduction to MoO_2 at 550–650°C, whereas the β-Mo_4O_{11} phase was formed at a temperature lower by 200 K under catalytic reaction conditions. This was likely due to the fact that, in the structure of rhombic MoO_3, the coordination of the Mo atom is intermediate between octahedral and tetrahedral with four neighboring atoms at a distance of 1.67–1.95 Å and two atoms at longer distances of 2.25 and 2.33 Å, which supplement the coordination to an octahedron. The rhombic phase of MoO_3 is considered as a structure consisting of MoO_4 tetrahedrons bound by oxygen vertexes to the nearest tetrahedrons. As a result, chains are formed along the c axis. In the structure of MoO_3, these chains are assembled in layers to increase the coordination number of Mo to five. In turn, the layers are arranged in pairs to form infinite packets with an increase in Mo coordination to six in a distorted octahedral structure [1, 11, 15].

Nucleation on reduction is characteristic of nonstoichiometric molybdenum oxides with the general formula Mo_nO_{3n-1} in the order $MoO_3 \longrightarrow MoO_2$; this nucleation leads to crystallographic shift structures rather than to the formation of vacancies [3]. Polyhedrons are joined with compression in a certain direc-

Table 2. Phase composition of multicomponent catalysts for isobutylene oxidation to methacrolein

Catalyst	Before operation				After operation			
	phase composition	d	I	I_1	phase composition	d'	I_2	I_3
$Co_8Mo_9Fe_3Bi_{0.75}O_x$	α-$CoMoO_4$	3.130	55	21	α-$CoMoO_4$	3.143	54	21
	β-$CoMoO_4$	3.356	100	39	β-$CoMoO_4$	3.371	100	39
	$Fe_2(MoO_4)_3$	3.857	38	14	$Fe_2(MoO_4)_3$	3.870	31	12
	$Bi_2O_3 \cdot MoO_3$	3.167	35	15	$Bi_2O_3 \cdot 2MoO_3$	3.180	36	14
	MoO_3	3.805	30	11	MoO_3	3.831	31	12
					β-Mo_4O_{11}	3.831	5	2
$Co_8Mo_{10}Fe_3Bi_{0.75}O_x$	α-$CoMoO_4$	3.128	62	23	α-$CoMoO_4$	3.143	84	27
	β-$CoMoO_4$	3.368	100	37	β-$CoMoO_4$	3.173	100	32
	$Fe_2(MoO_4)_3$	3.870	32	12	$Fe_2(MoO_4)_3$	3.877	28	9
	$Bi_2O_3 \cdot 2MoO_3$	3.178	52	19	$Bi_2O_3 \cdot MoO_3$	3.180	56	18
	MoO_3	3.818	28	9	MoO_3	3.811	34	11
					β-Mo_4O_{11}	3.931	8	3
$Co_8Mo_{11}Fe_3Bi_{0.75}O_x$	α-$CoMoO_4$	3.127	79	27	α-$CoMoO_4$	3.138	76	23
	β-$CoMoO_4$	3.358	100	34	β-$CoMoO_4$	3.371	100	30
	$Fe_2(MoO_4)_3$	3.867	38	13	$Fe_2(MoO_4)_3$	3.873	43	13
	$Bi_2O_3 \cdot MoO_3$	3.169	48	17	$Bi_2O_3 \cdot MoO_3$	3.178	49	15
	MoO_3	3.831	25	9	MoO_3	3.824	35	11
					β-Mo_4O_{11}	3.991	25	8
$Co_8Mo_{12}Fe_3Bi_{0.75}O_x$	α-$CoMoO_4$	3.125	78	25	α-$CoMoO_4$	3.136	76	22
	β-$CoMoO_4$	3.358	100	31	β-$CoMoO_4$	3.368	100	29
	$Fe_2(MoO_4)_3$	3.863	60	19	$Fe_2(MoO_4)_3$	3.873	54	16
	$Bi_2O_3 \cdot 3MoO_3$	3.180	55	17	$Bi_2O_3 \cdot 3MoO_3$	3.193	60	17
	MoO_3	3.776	25	8	MoO_3	3.831	38	11
					β-Mo_4O_{11}	4.003	18	5
$Co_8Mo_{13}Fe_3Bi_{0.75}O_x$	α-$CoMoO_4$	3.132	57	22	α-$CoMoO_4$	3.138	280	24
	β-$CoMoO_4$	3.361	100	39	β-$CoMoO_4$	3.368	100	31
	$Fe_2(MoO_4)_3$	3.853	35	14	$Fe_2(MoO_4)_3$	3.870	49	15
	$Bi_2O_3 \cdot 3MoO_3$	3.178	39	15	$Bi_2O_3 \cdot 2MoO_3$	3.178	57	17
	MoO_3	3.818	26	10	MoO_3	3.821	41	13
					β-Mo_4O_{11}	0	0	0
$Co_8Mo_{15}Fe_3Bi_{0.75}O_x$	α-$CoMoO_4$	3.127	55	19	α-$CoMoO_4$	3.136	56	19
	β-$CoMoO_4$	3.361	100	35	β-$CoMoO_4$	3.368	100	37
	$Fe_2(MoO_4)_3$	3.870	45	16	$Fe_2(MoO_4)_3$	3.877	38	13
	$Bi_2O_3 \cdot 3MoO_3$	3.182	49	17	$Bi_2O_3 \cdot 3MoO_3$	3.191	48	16
	MoO_3	3.798	34	13	MoO_3	3.834	35	11
					β-Mo_4O_{11}	3.987	0	0
$Co_8Mo_{12}Fe_3Bi_{0.75}O_x$ + K, SbO_y*	α-$CoMoO_4$	3.140	39	17	α-$CoMoO_4$	3.145	60	20
	β-$CoMoO_4$	3.358	100	43	β-$CoMoO_4$	3.373	100	34
	$Fe_2(MoO_4)_3$	3.857	34	15	$Fe_2(MoO_4)_3$	3.870	42	14
	$Bi_2O_3 \cdot MoO_3$	3.171	31	13	$Bi_2O_3 \cdot 3MoO_3$	3.195	38	13
	MoO_3	3.808	29	12	MoO_3	3.811	31	11
					β-Mo_4O_{11}	4.004	24	8
$Co_8Mo_{12}Fe_3O_x$	α-$CoMoO_4$	3.136	45	20	α-$CoMoO_4$	3.145	53	20
	β-$CoMoO_4$	3.366	100	45	β-$CoMoO_4$	3.371	100	37
	$Fe_2(MoO_4)_3$	3.870	46	20	$Fe_2(MoO_4)_3$	3.880	47	17
	MoO_3	3.821	33	15	MoO_3	3.824	37	14
					β-Mo_4O_{11}	3.927	32	12
$Co_8Mo_{12}Bi_{0.75}O_x$	α-$CoMoO_4$	3.123	62	26	α-$CoMoO_4$	3.140	66	24
	β-$CoMoO_4$	3.356	100	40	β-$CoMoO_4$	3.371	100	37
	$Bi_2O_3 \cdot 3MoO_3$	3.178	48	20	$Bi_2O_3 \cdot 3MoO_3$	3.191	53	19
	MoO_3	3.795	33	14	MoO_3	3.821	39	14
					β-Mo_4O_{11}	3.931	20	7

Note: d and d' are interplanar spacings corresponding to the most intense main line for samples before and after the reaction, respectively; I and I_1 are the intensities of the main line before and after operation, respectively, as percentages of the line intensity of β-$CoMoO_4$; I_2 and I_3 are the intensities of the main line before and after operation, respectively, as percentages of the total intensity.

* In this sample, the occurrence of an additional phase of a ternary compound like $Bi_2Fe_1Mo_2Fe_1O_{12}$ with d = 3.193 Å cannot be excluded.

tion. The appearance of a crystallographic shift conserves the phase with high structural organization but with a considerable deviation from stoichiometry. In this case, the neighboring octahedrons share not only vertexes but also edges. In the course of reduction, a situation occurs when the plane of oxygen ions disappears from the oxide surface and the neighboring rows of cations collectively migrate to octahedral holes. As a result, a plane of crystallographic shift appears on the surface of MoO_3 crystals and the subsequent cooperative diffusion results in the penetration of this plane from the surface deep into the crystal.

Knorr and Müller [16] supported the occurrence of mixed-valence Mo ions in the monoclinic phase of β-Mo_4O_{11}. In this structure, four independent molybdenum sites were detected; they are surrounded by both a tetrahedron (Mo_1) with similar Mo–O bond lengths (on average, 1.76 Å) and octahedral Mo_2–Mo_4. In the octahedral structure, bond lengths vary over a considerable range of 1.75–2.10 Å. This makes it possible to form a layered structure with molybdenum valence from five to six.

Distortions of this kind were also observed in another nonstoichiometric oxide modification—orthorhombic γ-Mo_4O_{11}, which also has four independent sites [17]. In this phase, distances in a tetrahedron, on average, are retained equal to 1.75–1.76, whereas the Mo–O bond length in an octahedron increases to 1.75–2.15 Å. The above suggests a labile structure of the main phase of MoO_3, which can easily lose oxygen, for example, for the formation of catalytic reaction products and a labile reduced oxide depending on conditions. Mixed-valence molybdenum and shear deformations facilitate the migration of molybdenum deep into the structure and the removal of oxygen in the course of a catalytic act. In our experiments on isobutylene oxidation, the nonstoichiometric β-Mo_4O_{11} phase was formed at much lower temperatures (as compared with the calcination of MoO_3) of 350–450°C, at which the catalytic reaction of olefin oxidation actively occurs.

Thus, a multiphase structure, which is required for the appearance of catalytic activity, is formed in the samples under the reaction conditions of olefin oxidation on complex Co–Mo–Bi–Fe catalysts. The β-$CoMoO_4$ phase occurs in combination with iron and bismuth molybdates and molybdenum oxides. The experimental results support our previous hypothesis [5] that the following two molybdenum oxide phases are formed under conditions of oxidative catalysis: reduced (Mo_4O_{11}) and oxidized (MoO_3) phases. The former phase, a crystallographic shift structure, can participate in the formation of an interface (plane) with iron molybdates on which catalysis takes place; the latter phase is in excess and does not participate in catalysis.

ACKNOWLEDGMENTS

This work was supported by the Russian Foundation for Basic Research (project no. 03-03-32228).

REFERENCES

1. Maksimov, Yu.V., Zurmukhtashvili, M.Sh., Suzdalev, I.P., Margolis, L.Ya., and Krylov, O.V., *Kinet. Katal.*, 1984, vol. 25, no. 5, p. 1164.
2. Shashkin, D.P., Shiryaev, P.A., Kutyrev, M.Yu., and Krylov, O.V., *Kinet. Katal.*, 1993, vol. 34, no. 2, p. 341.
3. Kihlborg, L.I., *Ark. Kemi*, 1963, vol. 21, p. 471.
4. Udalova, O.V., Shashkin, D.P., Shibanova, M.D., and Krylov, O.V., *Kinet. Katal.*, 2005, vol. 46, no. 4, p. 569 [*Kinet. Catal.* (Engl. Transl.), vol. 46, no. 4, p. 535].
5. Shashkin, D.P., Udalova, O.V., Shibanova, M.D., and Krylov, O.V., *Kinet. Katal.*, 2005, vol. 46, no. 2, p. 580 [*Kinet. Catal.* (Engl. Transl.), vol. 46, no. 2, p. 545].
6. Madeira, L.M., Portela, M.F., and Mazzocchia, C., *Catal. Rev.*, 2004, vol. 47, no. 1, p. 53.
7. Soares, A.P.V., Portela, M.F., and Kienemann, A., *Catal. Rev.*, 2004, vol. 47, no. 1, p. 125.
8. Kaddouri, A., Del Rossi, R., Mazzocchia, R., Gronchi, P., and Fumagalli, D., *J. Therm. Anal. Calorim.*, 2001, vol. 66, no. 1, p. 271.
9. Vierra, SoaresA.P., Farinha, PortelaM., Kienemann, A., Hilaire, L., and Miller, J.M.M., *Appl. Catal.*, 2001, vol. A206, no. 2, p. 221.
10. Li, J.-L., Zang, Y.-X., Liu, C.-W., and Zhu, K.-M., *Catal. Today*, 1999, vol. 51, no. 1, p. 195.
11. Syurakshin, A.V., *Cand. Sci. (Chem.) Dissertation*, Chernogolovka, Moscow oblast: Inst. of Problems of Chemical Physics, 2001.
12. Syurakshin, A.V., Savchenko, V.I., Krylov, O.V., and Knerel'man, E.I., *Neftekhimiya*, 2001, vol. 41, no. 3, p. 194 [*Pet. Chem.* (Engl. Transl.), vol. 41, no. 3, p. 175].
13. Plyasova, L.M., Zharov, V.I., Kustova, T.N., Karakchiev, L.T., and Andrushkevich, M.M., *Izv. Akad. Nauk SSSR, Neorg. Mater.*, 1973, no. 9, p. 519.
14. Smith, G.W. and Ivers, I.A., *Acta Cristallogr.*, 1965, vol. 19, part 2, p. 269.
15. Krilov, O.V., Maximov, Y.V.., and Margolis, L.Ya., *J. Catal.*, 1985, vol. 95, p. 289.
16. Knorr, R. and Müller, U., *Z. Anorg. Allg. Chem.*, 1995, vol. 621, p. 545.
17. Ghedira, M., Vincent, H., Marezio, H., Marcus, J., and Furcaudot, G., *J. Solid State Chem.*, 1995, vol. 56, p. 66.